ORIGINAL ARTICLE

Journal of Cachexia, Sarcopenia and Muscle (2021)
Published online in Wiley Online Library (wileyonlinelibrary.com) **DOI:** 10.1002/jcsm.12844

Extracellular vesicles derived from tumour cells as a trigger of energy crisis in the skeletal muscle

Fabrizio Pin[1,2], Marc Beltrà[1], Lorena Garcia-Castillo[1], Barbara Pardini[3,4], Giovanni Birolo[5], Giuseppe Matullo[5], Fabio Penna[1], Denis Guttridge[6,7] & Paola Costelli[1]*

[1]*Department of Clinical and Biological Sciences, University of Torino, Torino, Italy;* [2]*Department of Anatomy, Cell Biology and Physiology, Indiana University School of Medicine, Indianapolis, IN, USA;* [3]*Italian Institute for Genomic Medicine (IIGM), Candiolo, Italy;* [4]*Candiolo Cancer Institute, FPO-IRCCS, Candiolo, Italy;* [5]*Department of Medical Sciences, University of Torino, Torino, Italy;* [6]*Department of Cancer Biology, Ohio State University Comprehensive Cancer Center, Columbus, OH, USA;* [7]*Department of Pediatrics and Hollings Cancer Center, Medical University of South Carolina, Charleston, SC, USA*

Abstract

Background Cachexia, a syndrome frequently occurring in cancer patients, is characterized by muscle wasting, altered energy and protein metabolism and impaired myogenesis. Tumour-derived microvesicles (TMVs) containing proteins, messenger RNAs (mRNAs), and non-coding RNAs could contribute to cancer-induced muscle wasting.

Methods Differential ultracentrifugation was used to isolate TMVs from the conditioned medium of Lewis lung carcinoma and C26 colon carcinoma cell cultures. TMVs were added to the culture medium of C2C12 myoblasts and myotubes for 24–48–72 h, and the effects on protein and energy metabolism were assessed. TMVs were also isolated from the blood of C26-bearing mice. MicroRNA (miR) profile of TMVs was obtained by RNA-seq and validated by digital drop PCR. Selected miRs were overexpressed in C2C12 myoblasts to assess the effects on myogenic differentiation.

Results Differentiation was delayed in C2C12 myoblasts exposed to TMVs, according to reduced expression of myosin heavy chain (MyHC; about 62% of controls at Day 4) and myogenin (about 68% of controls at Day 4). As for myotubes, TMVs did not affect the expression of MyHC, while revealed able to modulate mitochondria and oxidative metabolism. Indeed, reduced mRNA levels of PGC-1α (C = 1 ± 0.2, TMV = 0.57 ± 0.06, normalized fold change, $P < 0.05$) and Cytochrome C (C = 1 ± 0.2, TMV = 0.65 ± 0.04, normalized fold change, $P < 0.05$), associated with increased BNIP3 expression (C = 1 ± 0.1, TMV = 1.29 ± 0.2, normalized fold change, $P < 0.05$), were observed, suggesting reduced mitochondrial biogenesis/amount and enhanced mitophagy. These changes were paralleled by decreased oxygen consumption (C = 686.9 ± 44 pmol/min, TMV = 552.25 ± 24 pmol/min, $P < 0.01$) and increased lactate levels (C = 0.0063 ± 0.00045 nmol/μL, TMV = 0.0094 ± 0.00087 nmol/μL, $P < 0.01$). A total of 118 miRs were found in MVs derived from the plasma of the C26 hosts; however, only three of them were down-regulated (RNA-seq): miR-181a-5p (−1.46 fold change), miR-375-3p (−2.52 fold change), and miR-455-5p (−3.87 fold change). No correlation could be observed among miRs in the MVs obtained from the blood of the C26 host and those released by C26 cells in the culture medium. Overexpression of miR-148a-3p and miR-181a-5p in C2C12 myoblasts revealed the ability to impinge on the mRNA levels of *Myf5*, *Myog*, and MyHC (*Myh4* and *Myh7*).

Conclusions These results show that in C2C12 cultures, TMVs are able to affect both differentiation and the mitochondrial system. Such effects could be related to TMV-contained miRs.

Keywords Cancer cachexia; Muscle wasting; Microvesicles; MicroRNAs; Mitochondria; Myogenesis

Received: 10 February 2021; Revised: 31 August 2021; Accepted: 30 September 2021
**Correspondence to: Paola Costelli, Department of Clinical and Biological Sciences, University of Torino, Corso Raffaello 30, 10125 Torino, Italy. Email: paola.costelli@unito.it*
Fabrizio Pin and Marc Beltrà contributed equally to the present study.

© 2021 The Authors. Journal of Cachexia, Sarcopenia and Muscle published by John Wiley & Sons Ltd on behalf of Society on Sarcopenia, Cachexia and Wasting Disorders. This is an open access article under the terms of the Creative Commons Attribution-NonCommercial License, which permits use, distribution and reproduction in any medium, provided the original work is properly cited and is not used for commercial purposes.

Introduction

Extracellular vesicles derived from cells of every type, including tumour cells, can be released in the circulation and convey functional information to distant sites. On the basis of their origin, size, physical properties, and functions, different types of extracellular vesicles have been described, among which exosomes and microvesicles (MVs).[1]

Exosomes (30–150 nm) form within the intraluminal vesicles generated in the multivesicular bodies as part of late endosomes. Multivesicular bodies can fuse with lysosomes for degradation or with the plasma membrane, releasing exosomes. Sorting of cargo during the internal budding of the membrane that leads to intraluminal vesicle formation is an essential step in exosome biogenesis.[1]

Microvesicle (0.1–1 μm) generation starts from the formation of outward buds in specific sites of the plasma membrane followed by fission and subsequent vesicle release into the extracellular space. In addition to rearrangements in the plasma membrane composition, proteins responsible for cell shape maintenance may be involved in MV biogenesis.[1]

Extracellular vesicle content consists, in variable proportions, of proteins, DNA, messenger RNAs (mRNAs), microRNAs (miRs), lipids, and surface molecules. In particular, miRs enclosed into extracellular vesicles are released into the bloodstream or other body fluids to transfer specific paracrine or endocrine messages thus altering gene expression of distant recipient cells.

Few observations suggest that extracellular vesicles are involved in the pathogenesis of cancer-induced muscle wasting.[2] Indeed, MVs derived from lung or pancreatic cancer cells induce myoblast apoptosis. These MVs contain miR-21 that, activating Toll-like receptor 7 on murine myoblasts, promotes apoptosis.[3] Exosomes produced by osteosarcoma cells have been shown to contain factors able to activate the notch-dependent signalling in muscle progenitors, resulting in impaired myogenesis.[4] More recently, muscle wasting in tumour-bearing mice has been shown to result from exosomal release of heat shock proteins,[5] while extracellular vesicles derived from Lewis lung carcinoma (LLC) cells have been reported to induce protein degradation in C2C12 myotubes and lipolysis in 3T3-L1 adipocytes.[6]

Muscle wasting, typically occurring in cancer patients, is one of the main features characterizing cancer cachexia, a complex syndrome associated with reduced survival, poor quality of life, and reduced tolerance to anticancer treatments.

Cancer-induced muscle protein depletion is mainly associated with hyperactivation of proteasome and lysosome-dependent degradation, although reduced protein synthesis occurs as well. Besides enhanced protein turnover, muscle wasting in cancer hosts also reflects an energy crisis mainly resulting from impaired oxidative capacity due to mitochondrial dysfunction.[7] Indeed, a proteomic profiling performed on the muscle of mice bearing the C26 colon carcinoma has shown an altered expression of proteins involved in energy homeostasis and mitochondrial function.[8] Consistently, mitochondria in the muscle of tumour-bearing animals display ultrastructural and functional changes,[8,9] ultimately resulting in decreased mitochondrial number and impaired oxidative capacity, as shown by reduced succinate dehydrogenase (SDH) activity and proportion of oxidative fibres in the muscle of tumour bearers.[9] Altered mitochondrial fusion, fission, and biogenesis, frequently associated with a pro-inflammatory environment, have also been reported.[10] Consistently with the observations above, markers of mitophagy and mitochondrial dynamics are altered in cachectic cancer patients, a picture that is further complicated by anticancer treatments.[11]

The mechanisms underlying muscle energy crisis in cancer cachexia are still unclear. The present study is aimed to investigate the occurrence of a causal connection among TMVs, muscle wasting, and derangements of energy metabolism in the skeletal muscle. The study demonstrates that the exposure to TMVs markedly affects myotube oxidative metabolism and that TMVs infused into healthy mice partially recapitulate some of the features of cancer cachexia.

Methods

Cell cultures

C2C12 and LLC cell lines were purchased from American Type Culture Collection, and C26 cells were obtained from Prof M. P. Colombo (National Cancer Institute, Milano, Italy). Yoshida AH-130 (AH-130) ascites hepatoma cells were a gift from Prof U. Del Monte (University of Milano, Italy). NIH-3T3 fibroblasts were kindly provided by Prof P. Porporato (University of Torino, Italy).

Murine C2C12, C26, LLC, and NIH-3T3 cells were cultured in Dulbecco's Modified Eagle Medium (DMEM) (Sigma-Aldrich) supplemented with 10% foetal bovine serum (FBS), 100 U/mL penicillin, 100 μg/mL streptomycin, 100 μg/mL sodium pyruvate, and 2 mmol/L L-glutamine and maintained at 37°C in a humidified atmosphere of 5% CO_2 in air. C2C12 myoblast differentiation was induced by shifting subconfluent cultures to DMEM supplemented with 2% horse serum (differentiation medium). For MV isolation, cells were maintained in either serum-free medium (C26, LLC) or 5% MVs-free FBS (NIH-3T3) for 48 h.

Plasmid cloning and cell transfection

Plasmids overexpressing miR-21-5p, miR-148a-3p, and miR-181-5p were designed and cloned using BLOCK-iT™ Pol II miR RNAi Expression Vector Kit (K4937, Invitrogen) following

DOI: 10.1002/jcsm.12844

manufacturer instructions. Plasmids were then transfected to either NIH-3T3 fibroblast or C2C12 myoblasts using Attractene Transfection Reagent (301005, Qiagen). Cells transfected with a plasmid coding for a SCR were used as control. The day after cell transfection, C2C12 myoblasts were shifted to differentiation medium and myogenic gene expression analysed after 2 and 4 days. As for NIH-3T3 fibroblasts, they were shifted to DMEM containing 5% MVs-free FBS. After 48 h, the conditioned medium was processed for MV isolation (3T3-MVs) as described below.

Animals

Experimental animals were cared for in compliance with the Italian Ministry of Health Guidelines (n°63/2014-B; 20/02/2014) and the Policy on Humane Care and Use of Laboratory Animals (NRC 2011). The experimental protocol was approved by the Bioethical Committee of the University of Torino. Male Wistar rats weighing approximately 150 g and Balb-c mice weighing approximately 20 g (Charles River Wilmington, MA) were maintained on a 12:12 h dark–light cycle with controlled temperature (18–23°C) and free access to food and water during the whole experimental period. Tumour-bearing mice (n = 8) were subcutaneously inoculated on the back with 5×10^5 C26 cells whereas tumour-bearing rats (n = 8) received an intraperitoneal inoculum of 10^8 AH-130 cells.

Tumour-bearing mice and rats were sacrificed under isoflurane anaesthesia 14 and 7 days after tumour transplantation, respectively. Total blood was obtained by cardiac puncture and processed to separate the plasma, subsequently stored at −80°C.

Microvesicle isolation

Microvesicles were isolated from (i) conditioned medium obtained from 250×10^6 C26 or LLC cells cultured for 48 h, (ii) plasma derived from healthy mice and rats, and (iii) plasma derived from C26 host or rats bearing the AH-130 hepatoma. Conditioned medium or plasma was centrifuged (300*g*, 10 min) to eliminate cell debris. The supernatant was recovered, and successive centrifugations at increasing speed were performed: one at 2000*g* for 20 min to eliminate dead cells, then one at 10 000*g* for 30 min to remove cell debris, and finally one at 100 000*g* for 70 min to pellet MVs. The resulting pellet was washed in phosphate-buffered saline (PBS) and ultracentrifuged again at the same speed (Supporting Information, *Figure* S1A). The pellet was resuspended in 1 mL PBS. Nanosight characterization of isolated particles revealed a population ranging from 90 to 600 nm, with a peak of abundancy at 200 nm (*Figure* S1B), thus confirming the enrichment in MVs.[12] MV internalization into C2C12 myotubes was assessed by fluorescence microscopy using the PKH26 fluorescent dye (Sigma-Aldrich).

Treatment with microvesicles

C2C12 myoblasts

Tumour-derived microvesicles were added to the culture medium of C2C12 myoblasts during 6 days from the beginning of differentiation. Within this period, cultures were analysed at 2, 4, and 6 days, roughly corresponding to differentiating myoblasts, early differentiated, and fully differentiated myotubes, respectively. Comparable experiments were performed exposing C2C12 myoblasts to 3T3-MV for 2 and 4 days after shifting to differentiation medium.

C2C12 myotubes

Fully differentiated C2C12 myotubes were treated with C26-derived or LLC-derived MVs for 24, 48, and 72 h.

In vivo studies

Healthy Balb-c mice were infused (i.v.) daily with a suspension of MVs derived from healthy mice or rats (used as controls) or from C26 tumour-bearing mice or AH-130 bearing rats. As for dosage, all the MVs obtained from 1.5 mL of blood (for both mice and rats) were infused each day in each animal.

Extracellular flux analysis

Mitochondrial oxygen consumption rate (OCR) was assessed by using the Mito-Stress Test Kit in a Seahorse XF Extracellular Flux Analyser (Agilent Technologies, Santa Clara, CA, USA) according to the manufacturer instructions. C2C12 myotubes were treated or not with LLC-MVs or C26-MVs for 24 h. One hour prior to assay, cultures were incubated in Seahorse XF Base Medium (Agilent Technologies) containing 1 mM Na-pyruvate, 2 mM glutamine, and 25 mM glucose in the absence of CO_2 supplementation for 1 h at 37°C. Basal respiration was monitored prior to addition of 2 μM oligomycin. The OCR values were obtained at baseline and after the addition of 2 μM oligomycin, 1 μM carbonyl cyanide 4-(trifluoromethoxy)phenylhydrazone), and 0.5 μM rotenone. OCR was automatically calculated and recorded by the Seahorse XF software (Agilent Technologies), and data were expressed as picomoles per minute.

Lactate assay

Lactate was measured in the cultured media of C2C12 myotubes treated or untreated with TMVs using the Lactate Colorimetric/Fluorimetric Assay kit (BioVision) according to the manufacturer's instructions.

DOI: 10.1002/jcsm.12844

Primary cultures

Balb-c mice were sacrificed under anaesthesia, and extensor digitorum longus and soleus muscles were rapidly excised and digested with type I collagenase (2 mg/mL, Sigma C0130) for 1 h at 37°C. Digested muscle were plated on matrigel-coated dishes (Sigma E1270) in DMEM supplemented with 20% FBS, 10% horse serum, 0.5% chick embryo extract, and 1% penicillin–streptomycin, allowing satellite cells release and attachment to the matrigel. Three days later, the medium was replaced with proliferation medium (DMEM 20% FBS, 10% horse serum, and 1% chick embryo extract). After 5 days, the medium was replaced with differentiation medium (2% horse serum and 0.5% chick embryo extract in DMEM). TMVs were added to primary cultures 48 h after the beginning of differentiation.

Protein synthesis

To assess the relative rate of protein synthesis, SUnSET methodology was used.[13] Briefly, 1 μM puromycin was added to the C2C12 culture medium 30 min before trypsinization. The amount of puromycin incorporated into nascent peptides was detected by western blotting, using a specific anti-puromycin antibody.

Western blotting

Total protein from C2C12 monolayers or from muscle tissues were extracted in RIPA buffer (50 mM Tris-HCl at pH 7.4, 150 mM NaCl, 1% NP40, 0.25% Na-deoxycholate, and 1 mM PMSF) with freshly added protease and phosphatase inhibitor cocktails, sonicated, and centrifuged at 3000*g* for 5 min at 4°C, and then the supernatant was collected. Protein concentration was assayed using BSA as working standard. Equal amounts of protein were heat denaturated in sample-loading buffer (50 mM Tris-HCl, pH 6.8, 100 mM DTT, 2% SDS, 0.1% bromophenol blue, and 10% glycerol), resolved by SDS-PAGE and transferred to nitrocellulose membranes (Bio-Rad). The filters were blocked with Tris-buffered saline containing 0.05% Tween and 5% non-fat dry milk and then incubated overnight with antibodies directed against: PGC-1 alpha (rabbit polyclonal antibody, Millipore), Cytochrome C (mouse antibody, BD Pharmingen), SDH-A (mouse monoclonal antibody Santa Cruz, CA), Caspase3 (rabbit polyclonal antibody, Sigma-Aldrich), myosin heavy chain (MyHC; mouse monoclonal antibody, clone MY32, Sigma-Aldrich), myogenin (mouse monoclonal antibody, clone F5D, Santa Cruz, CA), Pax7 (Developmental Studies Hybridoma Bank, University of Iowa), MyoD (rabbit polyclonal antibody, clone M318, Santa Cruz Biotechnology, CA), p-ERK (Thr202/Tyr204, rabbit monoclonal antibody, clone 20G111, Cell Signaling), ERK (goat polyclonal antibody, clone sc-94, Santa Cruz, CA), puromycin (mouse monoclonal antibody, clone 12D10, Millipore), and tubulin (mouse monoclonal antibody, clone T5168, Sigma-Aldrich). Peroxidase conjugated IgG (Bio-Rad) was used as secondary antibodies. Quantification of the bands was performed by densitometric analysis using a specific software (TotalLab, NonLinear Dynamics, Newcastle upon Tyne, UK).

Immunofluorescence

C2C12 monolayers were washed with PBS and fixed in 3% paraformaldehyde. Samples were then probed with the anti-MyHC antibody MF-20 (Developmental Studies Hybridoma Bank, Iowa City, IA, USA). Detection was performed using a fluorescein isothiocyanate-conjugated mouse or rabbit IgG secondary antibody. Nuclei were stained with Hoechst 33342 fluorochrome, and the images were captured using an epi-illuminated fluorescence microscope (Axiovert 35; Carl Zeiss MicroImaging GmbH, Jena, Germany).

MitoTracker Red CMXRos

Mitochondria polarization was assessed using the MitoTracker Red CMXRos selective probe (Molecular Probes, Barcelona, Spain). C2C12 cells were incubated in a medium without FBS and containing 100 nM MitoTracker for 30 min at 37 °C. The medium was then replaced with a complete medium without MitoTracker. Images were captured using an epi-illuminated fluorescence microscope (Axiovert 35; Carl Zeiss MicroImaging GmbH, Jena, Germany). Red CMXRos quantification was made by red fluorescence quantification. Myotubes were lysed on RIPA buffer (50 mmol/L Tris-HCl, pH 7.4, 150 mmol/L NaCl, 1% Nonidet P-40, 0.25% sodium deoxycholate, and 1 mmol/L phenyl-methylsulfonyl fluoride). After sonication, the lysate were centrifuged at 1500 *g* for 5 min. Supernatant fluorescence for Red CMXRos (∼579 nm excitation and ∼599 nm emission) and DAPI (∼358 nm excitation and ∼461 *nm* emission) was evaluated in a spectrofluorometer (Perkin-Elmer, Italy).

Real-time PCR

Total RNA was obtained using TriPure isolation reagent (Roche Applied Science, Indianapolis, IN) following the manufacturer's instructions. RNA concentration was determined fluorometrically using RiboGreen reagent (Invitrogen, Carlsbad, CA). RNA integrity was checked by electrophoresis on 1.2% agarose gel containing 0.02 mol/L morpholinopropanesulfonic acid and 18% formaldehyde. Total mRNA was retrotranscribed using an iScript cDNA synthesis kit (Bio-Rad Laboratories). Transcript levels were determined by real-time PCR using the SsoFast EvaGreen supermix and the

DOI: 10.1002/jcsm.12844

MiniOpticon thermal cycler (Bio-Rad Laboratories). Primer sequences (forward and reverse) were as follows:

1 *Bnip3* 5′-CAGAGCGGGGAGGAGAAC-3′ and 5′-GAGGCTGGAACGCTGCTC-3′;
2 *Sqtm1* 5′-CCCAGTGTCTTGGCATTCTT-3′ and 5′-AGGGAAAGCAGAGGAAGCTC-3′;
3 *Becn1* 5′-TGAAATCAATGCTGCCTGGG-3′ and 5′-CCAGAACAGTATAACGGCAACTCC-3′;
4 *Cycs* 5′-GGAGGCAAGCATAAGACTGG-3′ and 5′-TCCATCAGGGTATCCTCTCC-3′;
5 *Fbxo32* 5′-TCACAGCTCACATCCCTGAG-3′ and 5′-AGACTTGCCGACTCTTTGGA-3′;
6 *Trim63* 5′-TGTCTGGAGGTCGTTTCCG-3′ and 5′-ATGCCGGTCCATGATCACTT-3′;
7 *Ppargc1a* 5′-GCCAAAGCTGAAGCCCTCTTG-3′ and 5′-TGCAAGGAGAGACCTGCTTGCT-3′
8 *Myf5* 5′-TGAAGGATGGACATGACGGACG-3′ and 5′-TTGTGTGCTCCGAAGGCTGCTA-3′;
9 *Mef2c* 5′-AGATCTGACATCCGGTGC-3′ and 5′-TCTTGTTCAGGTTACCAGCT-3′;
10 *Myog* 5′-GCAAATGATCTCCTGGGTTG-3′ and 5′-ATCCAGTACATTGAGCGCCT-3′;
11 *Myh4* 5′-CACCTGGACGATGCTCTCAGA-3′ and 5′-GCTCTTGCTCGGCCACTCT-3′;
12 *Myh7* 5′-CTCAAGCTGCTCAGCAATCTATTT-3′ and 5′-GGAGCGCAAGTTTGTCATAAGT-3′

For mature miR analysis, all miRs were retrotranscribed using the miScript II RT Kit (Qiagen, Hilden, Germany). Transcript levels were determined by quantitative real-time PCR using the miScript SYBR Green PCR Kit (Qiagen, Hilden, Germany) and the CFX Connect Real-Time PCR Detection System (Bio-Rad, Hercules, CA, USA). Fifteen seconds of denaturation at 95°C were followed by 30 s of annealing at 55°C and extension at 70°C for 30 s. These steps were repeated for 40 cycles. A universal primer was used together with a miR specific primer in each reaction (miScript Primer Assay, Qiagen, Table 3). For samples with low amount of total RNA, a step of pre-amplification was added before real-time quantification by using the miScript PreAMP PCR Kit (Qiagen, Hilden, Germany) in combination to a selection of miR specific primers. Every quantitative real-time PCR was validated by analysing the respective melting curve. Gene expression were normalized to either SNORD72 expression or the mean of a group of selected housekeeping miRs (let-7i-5p, miR-27b-3p, and miR-152-3p), and results are expressed as $-\Delta Ct$.

Small RNA-sequencing

Total RNA concentration was quantified by Qubit® 2.0 Fluorometer with Qubit® microRNA Assay Kit (Invitrogen, Carlsbad, CA, USA). Small RNA transcripts were converted into barcoded cDNA libraries. Library setting was performed using NEBNext Multiplex Small RNA Library Prep Set for Illumina (New England BioLabs Inc., Ipswich, MA, USA). Each library was prepared with a unique indexed primer, according to previous studies.[14] The obtained sequence libraries were subjected to the Illumina sequencing pipeline, passing through clonal cluster generation on a single-read flow cell (Illumina Inc., San Diego, CA, USA) by bridge amplification and were sequenced at ultrahigh throughput on NextSeq500 (Illumina Inc., San Diego, CA, USA). One flowcell in 24-plex could produce about six million single reads per sample, 75 base pairs long. Sequencing results were validated using digital PCR. Housekeeping genes were chosen following a modified version of the methodology described by Eisenberg and Levanon.[15]

Bulk small RNA-sequencing (sRNA-Seq) on MVs isolated from C26 cell cultures and from the plasma of C26-bearing mice was performed. The expression of small non-coding (snc)RNAs in the skeletal muscle was analysed using two library sets originating from two different animal experiments, referred to as ML-1 and ML-2. As for plasma MVs, library was prepared on material contained in MVs isolated from the plasma of ML-2 animals. In this particular case, only $n = 4$ controls reached the minimal RNA concentration needed and were loaded for sequencing, while all $n = 6$ C26 samples were sequenced. Additionally, we included the sequencing of three samples containing MVs isolated from the culture medium of C26 cells in step-down condition. All libraries were run at the same sequencing facility, and bioinformatic analysis was performed by the same operator, following the pipeline represented in *Figure* S1C. Raw sequencing data were deposited on Gene Expression Omnibus with the identifier GSE165531 (token for Reviewer access: slobyoauntyrtkx).

Digital PCR

The expression of miRs in plasma-derived MVs was quantified by means of the QX200 TM Droplet Digital TM PCR System (ddPCR, Bio-Rad) using EvaGreen Digital PCR Supermix (Bio-Rad) with Droplet Generation Oil for EvaGreen (Bio-Rad) following manufacturer's instruction. Briefly, 20 μL of EvaGreen Supermix, 2 μM primers, and pre-amplified cDNA were transferred in a droplet generation cartridge and mixed with 70 μL of droplet generation oil to obtain an emulsion. Droplets (40 μL) were transferred to a new ddPCR 96-well plate. Amplification of specific miRs was obtained with the following protocol: 95°C 5 min 1 cycle enzyme activation, 95°C 30 s 40 cycles denaturation, 54°C 1 min 40 cycles annealing/extension, 4°C 5 min 1 cycle signal stabilization, 90°C 5 min 1 cycle signal stabilization, 4°C 40 min 1 cycle, 4°C. Fluorescence of single droplets was read using QX200 Droplet Reader, and data were analysed using the QuantaSoft

DOI: 10.1002/jcsm.12844

Version 1.7.4 Software (Bio-Rad) and expressed in copy number per microlitre.

Data analysis and presentation

Data are expressed as means ± SD, with the exception of gene expression (means ± SEM). The significance of the differences was evaluated by Students *t*-test or ANOVA followed by uncorrected Fisher's least significant difference. sRNA-Seq pipeline analyses were performed using a methodology described in Sabo *et al*.[14]

Results

Tumour-derived microvesicles affect C2C12 myoblast differentiation

C2C12 myoblast were exposed to TMVs derived from C26-MVs or LLC-MVs conditioned medium starting from the beginning of differentiation (Day 0) and analysed after 2, 4, and 6 days, roughly corresponding, respectively, to differentiating myoblasts, early, and fully differentiated myotubes. In comparison with untreated cultures, the morphological appearance of C2C12 cells treated for 2 and 4 days with MVs suggested a delayed differentiation no longer appreciable after 6 days (*Figure* 1A). A comparable pattern was observed in primary cultures of muscle progenitors isolated from both the soleus and the extensor digitorum longus muscles of healthy mice exposed to C26-MVs for 24 and 48 h (*Figure* S2A and S2B).

The delayed differentiation was partially consistent with the expression of molecules driving myogenesis. Indeed, myogenin, a marker of late differentiation, is down-regulated with respect to control values at Days 4 and 6 (*Figure* 1B and 1C) while unchanged Pax7 and MyoD levels were detected throughout the experiment (*Figure* 1B and 1C). Differentiating C2C12 myoblast did not die by apoptosis, as demonstrated by both the morphological appearance (*Figure* 1A) and the lack of activated caspase-3 after exposure to C26-MVs/LLC-MVs at any time point (*Figure* 1D). Previous observations showed that muscle wasting in C26-bearing mice was associated with impaired myogenesis and could be corrected by MEK inhibitors.[16,17] Consistently, the results reported in *Figure* 1B and 1C show a trend to increase of the p-ERK/ERK ratio in C2C12 myoblasts exposed to both C26-MVs and LLC-MVs with respect to control cultures.

The expression of MyHC paralleled the morphological data, being lower in TMV-treated cultures than in control

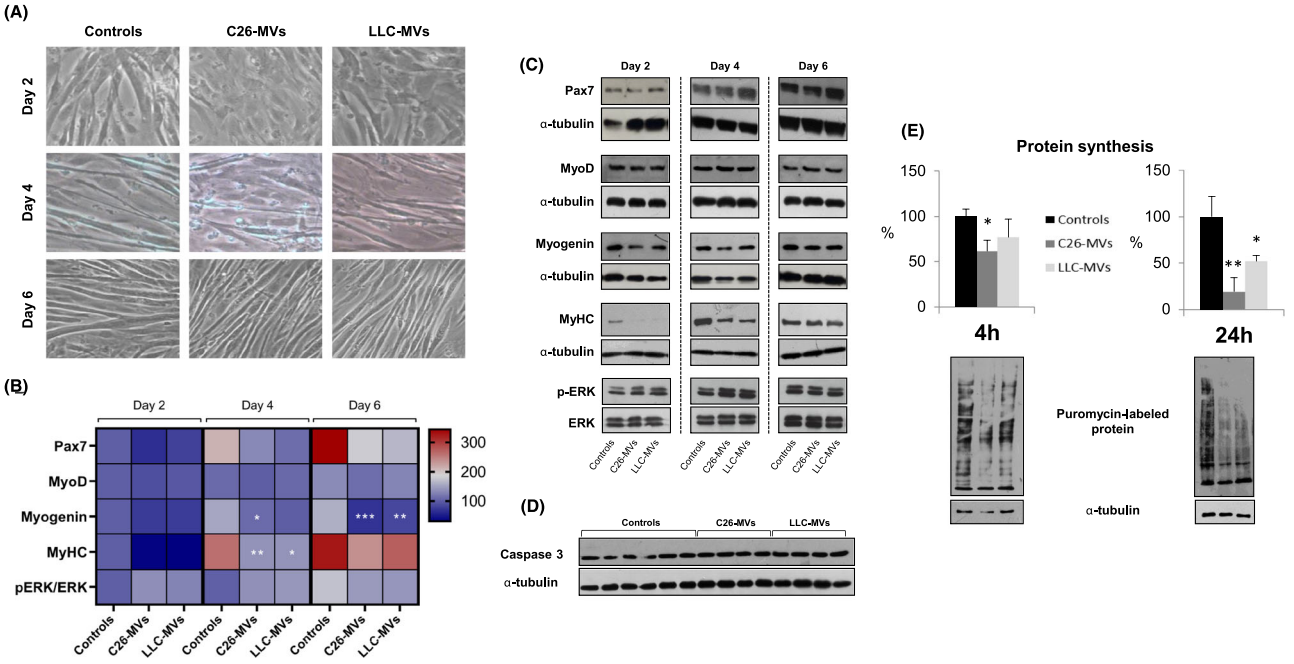

Figure 1 Effect of tumour-derived microvesicles on C2C12 myoblast differentiation. (A) Phase-contrast microscopy of C2C12 myoblast cultures during differentiation in the presence or in the absence of C26-MV or LLC-MV (scale bar: 100 μm); (B) heat map representing changes in protein expression. Data are expressed as arbitrary units (AI); $n = 3$ for each experimental condition, statistical significance is set at $P < 0.05$; (C) representative western blotting pattern of protein expression reported in panel (B); (D) western blotting showing caspase-3 expression; (E) representative blots and quantification of Sunset analysis for the assessment of protein synthesis 4 and 24 h after exposure to C26-MV or LLC-MV. Data are expressed as % of controls, $n = 3$. Significance of the differences: $^{*}P < 0.05$, $^{**}P < 0.01$ vs. controls. LLC, Lewis lung carcinoma; MV, microvesicles.

DOI: 10.1002/jcsm.12844

cells at 2 and 4 days after differentiation, still showing a non-significant trend to reduction at Day 6 (*Figure* 1B and 1C). Reduced MyHC levels were associated with decreased *de novo* protein synthesis (*Figure* 1E), C26-MVs appearing more effective than LLC-MVs (*Figure* 1E).

Remodelling of the mitochondrial network is an important step during myogenic differentiation.[18] Along this line, the impact of TMVs on mitochondria during C2C12 differentiation was assessed. The amount of polarized mitochondria was reduced in differentiating C2C12 cultures exposed to TMVs (*Figure* S3A). The expression of PGC-1α, the master regulator of mitochondrial biogenesis, was unchanged at all the experimental points (*Figure* S3C), although a not significant trend towards reduction could be envisaged. SDH-A expression was significantly reduced at Day 6 (*Figure* S3B), indicating a reduced mitochondrial function.

Tumour-derived microvesicles modulate energy metabolism in C2C12 myotubes

To assess if TMVs could affect mature myotubes, fully differentiated C2C12 cultures were exposed to C26-MVs or LLC-MVs for 24 h. *Figure* S4A demonstrates that both TMVs were able to directly interact with and enter C2C12 myotubes.

Immunostaining for MyHC showed that myotube size was not affected by C26-MVs or LLC-MVs (*Figure* 2A). Consistently,

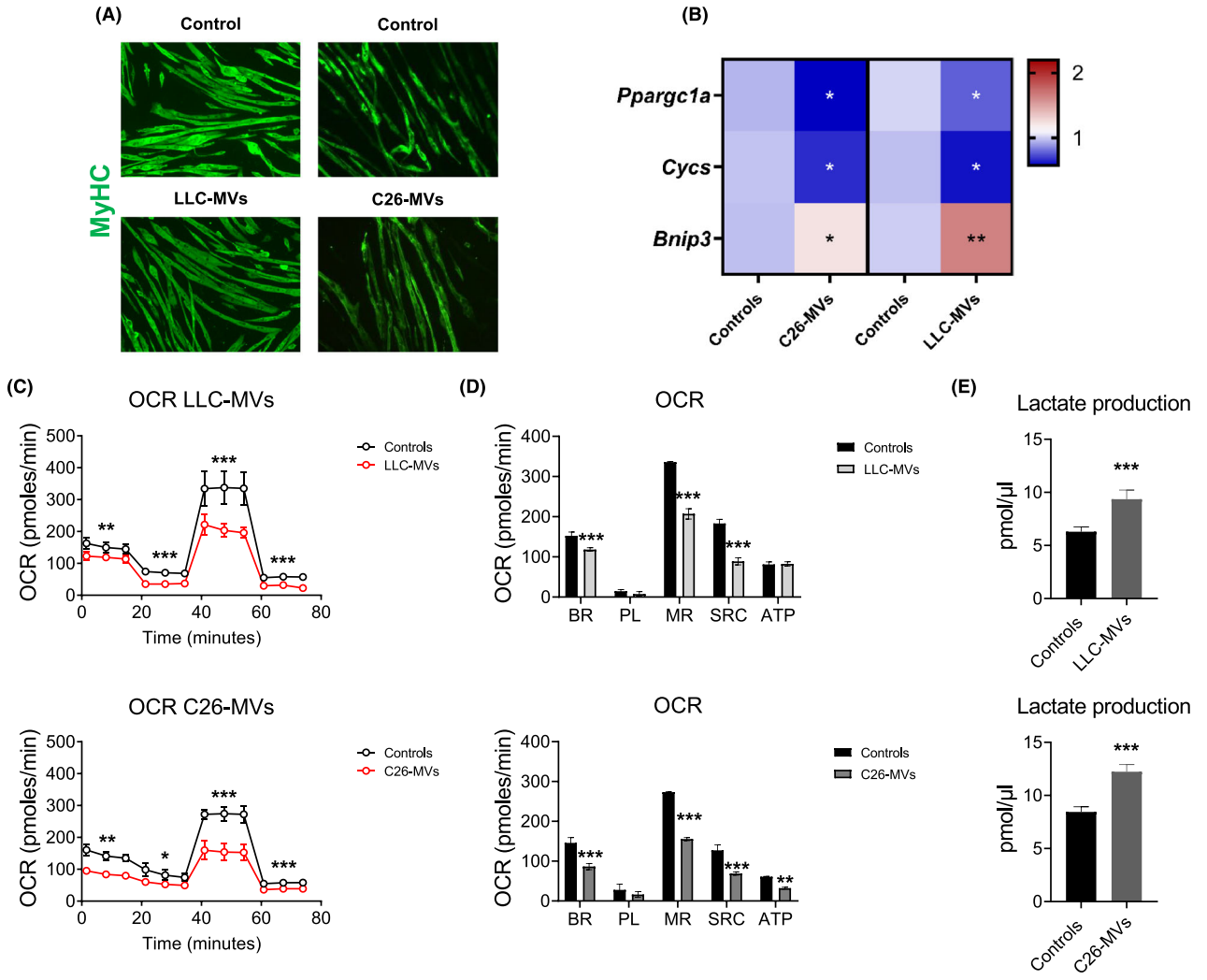

Figure 2 Effect of tumour-derived microvesicles on C2C12 myotubes. (A) Immunofluorescence analysis of MyHC expression after 24 h of tumour-derived microvesicle exposure; (B) heat map (ΔΔCt; *n* = 3) showing the expression of mitochondria-related genes. (C–D) Mitochondrial respiration and oxygen consumption rate (OCR) in C2C12 myotubes exposed to LLC and C26-MVs for 24 h (*n* = 3). ATP, adenosine triphosphate; BR, basal respiration; MR, maximal respiration; PL, proton leak; SRC, spare respiratory capacity. Data expressed as picomoles per minute. (E) Lactate release from C2C12 myotubes exposed to LLC-MVs or C26-MVs. Data are expressed as means ± SD, *n* = 3. Significance of the difference: $*P < 0.05$, $**P < 0.01$, $***P < 0.001$ vs. controls.

DOI: 10.1002/jcsm.12844

the mRNA levels of *Fbxo32/Atrogin1 and Trim63/Murf1*, muscle-specific ubiquitin ligases frequently up-regulated in myotubes exposed to catabolic stimuli, remained comparable to control values (normalized fold change 24–48 h: C = 1; C26-MV = 1.13–1.40; LLC-MV = 1.08–0.99).

In order to evaluate the effects of TMVs on mitochondria homeostasis, markers of mitochondrial biogenesis and function were analysed. As shown in *Figure* 2B, the mRNA expression of both *Ppargc1a and Cycs* was reduced after 24 h exposure to C26-MVs or LLC-MVs when compared with untreated myotubes. By contrast, the expression of *Bnip3*, a molecule involved in mitophagy, which is the leading mechanism for the disposal of dysfunctional mitochondria, was increased. Such a pattern was associated with reduced amount of polarized mitochondria, at least in myotubes exposed to C26-MVs (*Figure* S4B). Consistently, a significant impairment of mitochondrial respiration occurred (*Figure* 2C). Both LLC-MVs and C26-MVs were able to reduce basal respiration, maximal respiration, and spare respiratory capacity (*Figure* 2D). Only the C26-MVs negatively modulated the ATP production that was unchanged in the presence of LLC-MVs (*Figure* 2D). Furthermore, TMVs stimulated lactate release into the culture medium of C2C12 myotubes (*Figure* 2E), suggesting a shift from oxidative to glycolytic metabolism.

Microvesicles isolated from the plasma of tumour-bearing animals partially recapitulate cachexia in healthy mice

The ability of the MVs derived from the plasma of tumour-bearing mice in reproducing cachexia in healthy animals was assessed. MVs isolated from C26 hosts and rats bearing the AH-130 hepatoma, a tumour known to rapidly induce cachexia in the host,[19] were infused into healthy mice with daily i.v. injection for a maximum of 4 days. As shown in *Figure* 3, MV infusion resulted in slightly reduced GSN mass in comparison with controls. A different kinetic was observed among animals infused with C26-MVs (*Figure* 3A) or AH130-MVs (*Figure* 3C). As for the tibialis anterior, only AH130-MVs led to a reduction in size (*Figure* 3B and 3D).

The expression of genes involved in mitochondrial homeostasis and protein degradation did not change in the GSN of mice receiving MVs from the C26 host, with the exception of increased *Becn1/Beclin1* levels (*Figure* S5A). When mice were treated with AH130-MVs for 72 h, *Ppargc1a* expression did not change, whereas *Cycs* was reduced. Similarly, the levels of both *Bnip3* and *Trim63/Murf1* were reduced, while no differences could be observed as for *Fbxo32/Atrogin1*, *Becn1/Beclin1*, and *p62/Sqstm1*. By contrast, most of these

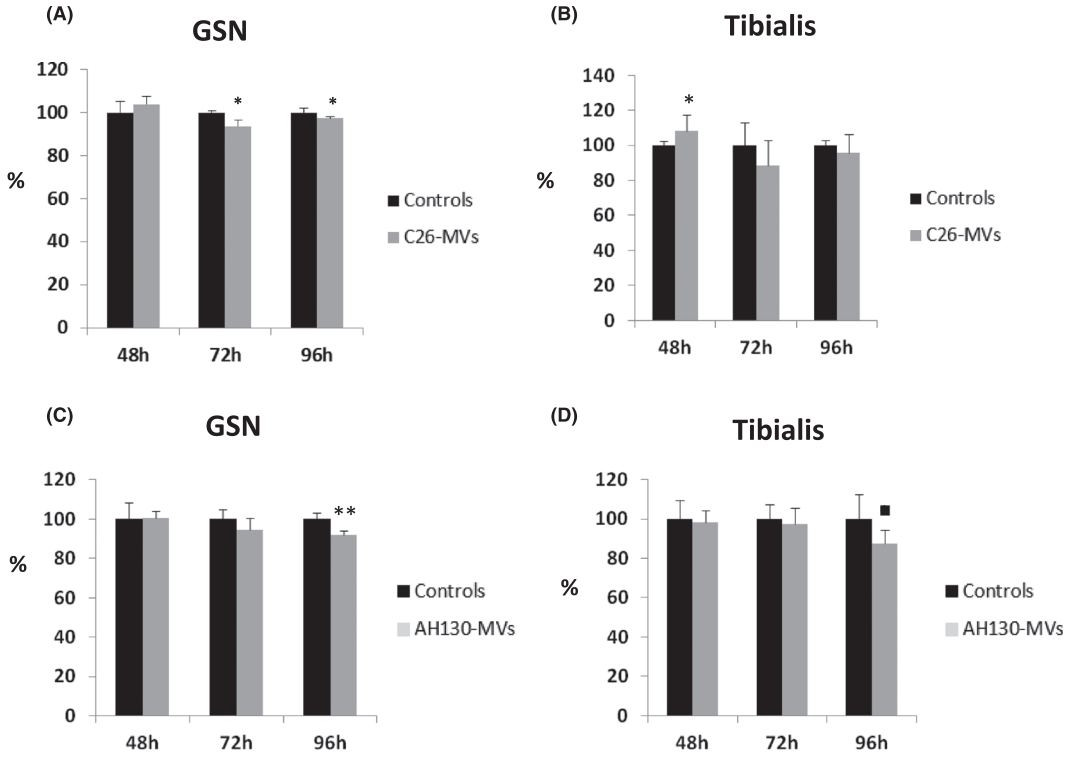

Figure 3 Tumour-derived microvesicles infused into healthy mice partially recapitulate cachexia. Changes in (A, C) gastrocnemius and (B, D) tibialis anterior mass in healthy mice infused for 48, 72, and 96 h with C26-MV or AH130-MV. Data (mg/10 g initial body weight, means ± SD) are expressed as % of controls, $n = 5$. Significance of the differences: $^{*}P < 0.05$, $^{**}P < 0.01$ vs. controls. MV, microvesicles.

DOI: 10.1002/jcsm.12844

markers were overexpressed in comparison with untreated animals at 96 h, with the exception of *atrogin-1* and *beclin-1* that remained unchanged (*Figure* S5B).

Tumour-derived microvesicles show a peculiar small non-coding RNA profile

Tumour-derived microvesicles are one of the routes by which tumour cells convey signals to both surrounding and distant target tissues. In this study, the attention was focused on sncRNAs by analysing MVs isolated from the plasma of the C26 hosts (*Figure* 4) and from C26 culture medium (*Figure* 5) by sRNA-Seq.

Plasma MV samples showed poor group clustering in principal component analysis, indicating high sample variability (*Figure* 4A and 4B). Although MV content was represented mostly by miRs (86.93% of reads aligned to miRs), MV cargo was further enriched with other types of sncRNAs such as lincRNAs (2.20%), rRNAs (1.87%), snRNAs (1.73%), and snoRNAs (1.43%), along with high diversity of sequences for each biotype (*Figure* 4B). Up to 122 different miR sequences were detected in plasma MVs, the top 20 being reported in *Figure* 4C. From all the detected miRs, only miR-181a-5p, miR-375-3p, and miR-455-5p were significantly down-regulated in MVs isolated from the plasma of the C26 hosts with respect to those deriving from healthy, control mice (*Figure* 4D). Although the average fold changes were high for other miRs, sample variance in both control mice and C26 hosts compromised statistics assessment, as exemplified by miR-1a-3p and miR-21a-5p expression (*Figure* 4E). Indeed, while miR-21a-5p is not significant when correcting for multiple testing, it is nominally significant ($P = 0.005$) and still one of the top miRs (#7), so with a larger sample size changes would likely be significant. By contrast, miR-1a-3p is weaker and not nominally significant (although close to, P value being 0.057). Additionally, other myomiRs such as miR-133a-3p and miR-206-3p, which were described to be modulated in the blood of patients suffering from different myopathies,[20] were detected in very low amounts and apparently not altered in the present experimental setting (*Figure* 4E). Among the three miRs found significantly modulated, validation by digital droplet PCR confirmed the down-regulation just for miR-375-3p (*Figure* S6).

Microvesicles isolated from the plasma of the C26-bearing mice are produced by both tumour and host cells. In terms of miR content, the differences observed between MVs obtained from tumour-bearing and control mice could reflect the contribution of the C26 cells but also host cell response to the tumour. To investigate this point, sncRNA cargo was assessed in MVs released in C26 culture medium, showing that they contained several let-7 family members as well as

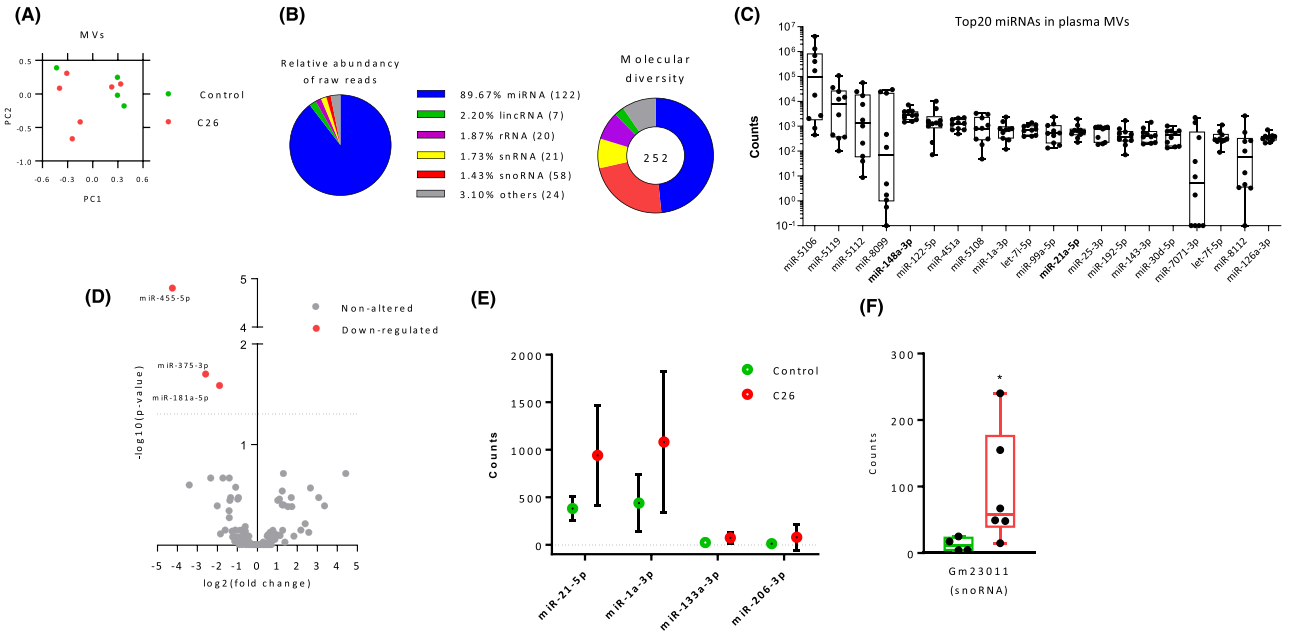

igure 4 F miR expression profile in circulating MVs of C26-bearing mice. (A) PCA plot (PC1 vs. PC2) representing sample variability in the library; (B) raw read abundance and molecular diversity of each sncRNA biotype; (C) top 20 miRs detected in circulating MVs; (D) volcano plot reporting all detected miRNAs in the gastrocnemius, according to P value (−log10) and fold change (log2) distribution (controls: $n = 4$; C26: $n = 5$). Significance of the difference set at $P < 0.05$; (E) expression of selected myomiRs in the gastrocnemius of controls and C26 hosts (means ± SEM); (F) panel representing the changes in the levels of the snoRNA Gm23011 in the gastrocnemius of the C26 hosts. For all 'box and whisker' plots, data are represented as: line = median, whiskers = min to max (controls: $n = 4$; C26: $n = 5$; $P < 0.05$). miR, microRNA; MV, microvesicles.

DOI: 10.1002/jcsm.12844

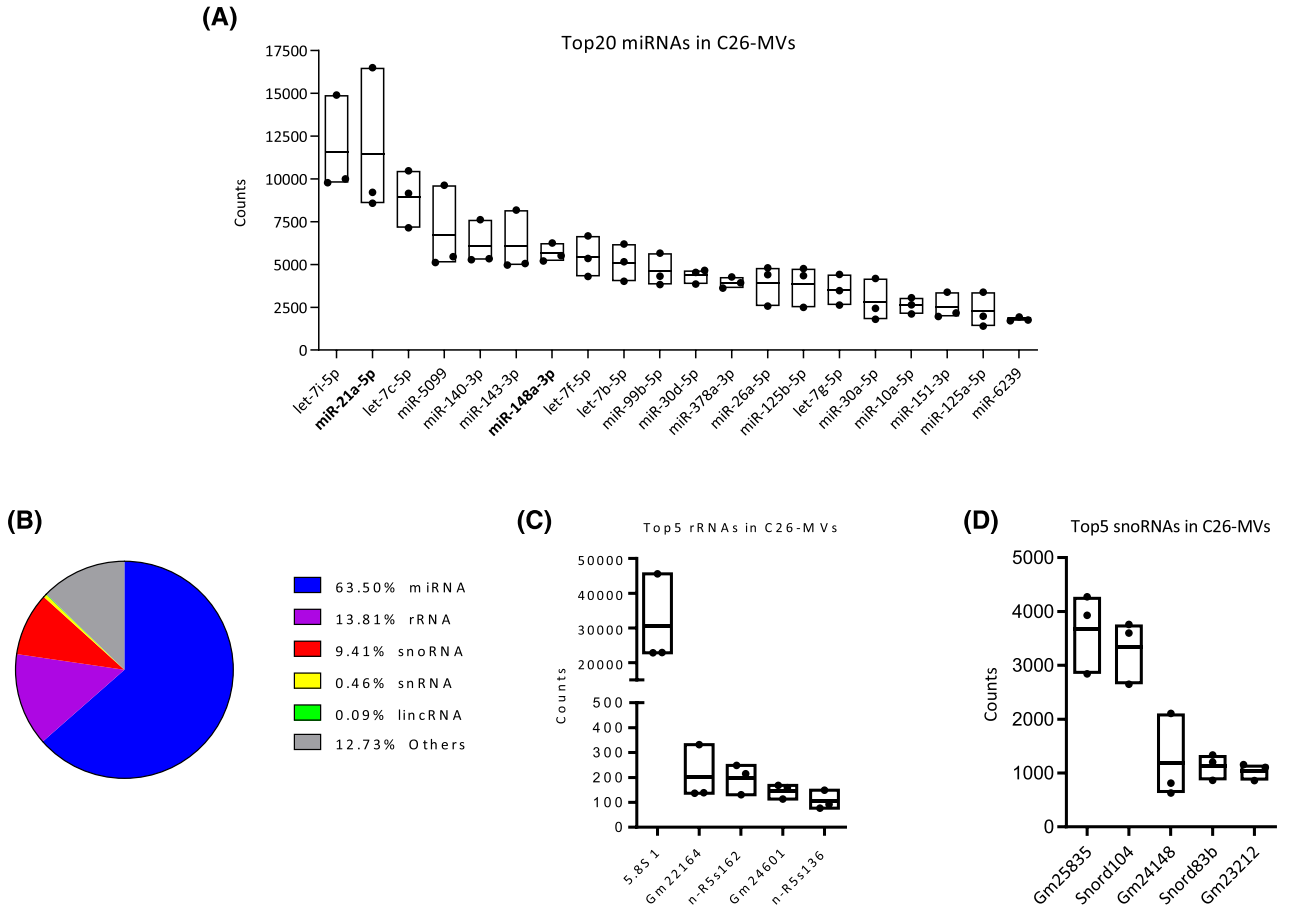

Figure 5 miR expression profile in MVs isolated from the C26 CM. (A) Top 20 miRs detected in MVs isolated from the C26 CM; (B) molecular diversity of each sncRNA biotype; (C) top 5 rRNAs and (D) top 5 snoRNAs in MVs isolated from the C26 CM. For all 'box and whisker; plots, data are represented as: line = median, whiskers = min to max (n = 3). miR, microRNA; MV, microvesicles.

miR-21a-5p (*Figure* 5A). C26-MVs also contained large number of miR-148a-3p reads. By contrast, low read counts for miR-181a-3p (mean counts = 127) were collected, while both miR-375-5p and miR-455-5p were absent (*Figure* 5A). Despite these results suffer from the limitation of lacking an appropriate control, for example, normal enterocytes, they reasonably demonstrate that the down-regulation of miR-181a-5p, miR-375-3p, and miR-455-5p observed in MVs isolated from the plasma of the C26 hosts unlikely reflects the contribution of MVs released by the tumour cells. However, as an additional consideration and note of care, the possibility that the C26 cells could release MVs with different miR content *in vitro* and *in vivo* cannot be discarded.

Besides miRs, the sRNA-Seq data set used in the present study also included annotations for several other types of sncRNA, including snoRNAs, mt-tRNAs, snRNAs, and rRNAs among the other biotypes (*Figure* 5B). As for plasma-derived MVs, only Gm23011, a sequence predicted to be a snoRNA (Ensambl entry: ENSMUST00000104148.3), was found up-regulated in MVs isolated from C26 hosts compared with controls (*Figure* 4E). *Figure* 5C and 5D shows the top 5 rRNAs and snoRNAs, respectively, in MVs isolated from C26 CM.

MicroRNAs contained into microvesicles isolated from cultured C26 cells slightly impinge on myogenesis

C2C12 myoblasts were either transfected with plasmids overexpressing miR-21-5p, miR-148a-3p, and miR-181-5p or exposed to MVs isolated from NIH3T3 fibroblasts overexpressing the same miRs (3T3-MVs; refer to Methods section), and the effects on markers of myogenesis were evaluated. The results reported in *Figure* 6 show that overexpressing miR-148a-3p into C2C12 myoblasts resulted in increased mRNA levels of *Myf5* and *Myog* at Day 2 of differentiation, although not at Day 4. By contrast, overexpressing miR-181a-5p reduced the mRNA levels of genes coding for MyHC, namely, *Myh4* and *Myh7*. Decreased levels of *Myh7* were observed also in C2C12 cells overexpressing miR-21-5p

DOI: 10.1002/jcsm.12844

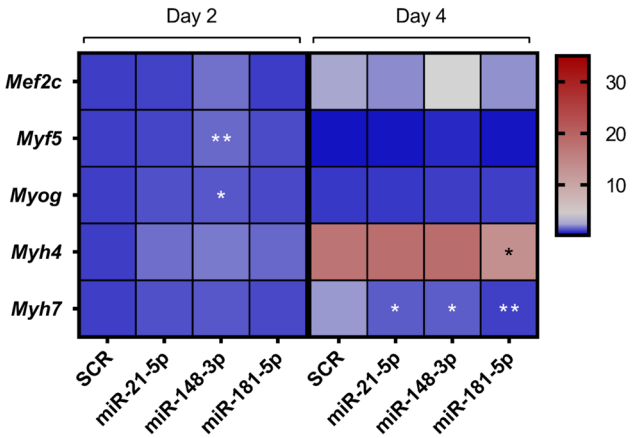

Figure 6 Effect of miRs contained into C26-MVs on the expression of genes involved in myogenesis. (A) Heat map (ΔΔCt; $n = 3$) showing the expression of genes involved in C2C12 overexpressing specific miRs at Days 2 and 4 of differentiation. Significance of the differences: $^{*}P < 0.05$, $^{**}P < 0.01$ vs. SCR (scramble) for each time point. SCR, scrambled sequence.

or miR-148a-3p at Day 4 of differentiation. These observations are partially consistent with the reduced MyHC protein levels observed in differentiating C2C12 cultures (refer to *Figure* 1B). No appreciable effect could be detected in C2C12 cultures exposed to 3T3-MVs (data not shown).

Discussion

This is the first study reporting that MVs secreted from tumour cells impair differentiation of murine myoblasts *in vitro* and significantly affect energy metabolism in myotube cultures. Moreover, MVs isolated from the plasma of tumour-bearing animals partially recapitulate cachexia when infused into healthy animals.

The first relevant observation reported in the present study is that cytotoxicity does not occur in TMV-exposed C2C12, in contrast with results reported by He *et al.*[3] This latter study is performed adding TMVs to myoblasts maintained in growing medium, while the results here presented refer to cultures in differentiating medium (refer to Methods section), suggesting that growing, but not differentiating, myocytes are prone to TMV-induced cytotoxicity. Indeed, myotubes were reported to be more resistant than myoblasts to death, due to enhanced anti-apoptosis pathways driven by apoptosis repressor with caspase recruitment domain, HSP70, and HSP25.[21] In addition, recent observations showed that both apoptosis induction and apoptosome assembly are required for myoblast differentiation.[22] In this regard, the apoptotic stimulus provided by TMVs could likely result in cell death only when applied to proliferating myoblasts.

Tumour-derived microvesicle exposure in differentiating C2C12 cultures results in delayed, although not inhibited, shift from myoblasts to myotubes, as demonstrated by the morphologic analysis, by the steadily reduced levels of myogenin and by the transient decrease of MyHC expression. To the best of our knowledge, this is the very first evidence that TMVs can impinge on *in vitro* myogenesis. There are just few studies published on this topic. Extracellular vesicles isolated from C2C12 myotubes exposed to pro-oxidant agents impaired myoblast differentiation.[23] Alternatively, extracellular vesicles derived from mesenchymal stem cells, endothelial, and inflammatory cells were required for an efficient muscle regeneration.[24] In the present study, the delayed myogenic differentiation induced by TMVs is associated with reduced protein synthesis and with a trend to increased levels of the p-ERK/ERK ratio. This latter, in particular, suggests a consistency with previous observations showing that increased p-ERK levels in the muscle of the C26 hosts, causally contributed to wasting also by impinging on regeneration.[16] In addition, increased p-ERK levels were reported in TNFα-treated myoblast cultures, characterized by delayed differentiation.[16] The possibility that TMVs could delay myoblast differentiation by releasing TNFα is unlikely because C26 cells do not produce this cytokine in significant amounts.[25]

In addition to modulate *in vitro* myogenic differentiation, TMVs also impinge on energy metabolism in myotube cultures, by reducing mitochondrial respiration and increasing lactate production. Such functional alterations are paralleled by reduced expression of proteins involved in mitochondrial biogenesis/content and by increased levels of the marker of mitophagy *Bnip3*. These observations do not conform to the data available in the literature. Indeed, extracellular vesicles derived from mesenchymal stem cells infused into mice with kidney injury were reported to improve mitochondrial antioxidant defence and ATP production, to reduce mitochondrial fragmentation and to preserve both mitochondrial membrane potential and mitochondrial number.[26] Exosomes derived from endothelial progenitors added to homotypic cells exposed to hypoxia and reoxygenation were shown to decrease mitochondrial fragmentation and to elevate mitochondrial membrane potential and ATP levels.[27] Extracellular vesicles isolated from a hippocampal cell line exposed to TNFα were able to increase the mitochondrial OCR in naive cells. However, also proton leak and the production of reactive oxygen species were enhanced, suggesting that, despite the improved oxidative phosphorylation, mitochondria were not properly working.[28] Finally, extracellular vesicles derived from C2C12 myotube cultures suppressed the enhanced oxygen consumption and mRNA expression of markers of mitochondrial biogenesis induced by RANKL in murine bone marrow cells and preosteoclastic Raw264.7 cells.[29] Consistently with this last observation, the results reported in the present study demonstrate that TMVs exert a negative action on mitochondrial function in C2C12 myotube cultures, supporting their contribution to energy crisis in tumour-bearing mice. Consistently, exposure to TMVs

DOI: 10.1002/jcsm.12844

partially recapitulates cachexia in healthy mice. However, depending on the host by which MVs are derived (C26 or AH-130 bearing mice), this cachexia-inducing effect differently impinges on the expression of genes involved in mitochondrial homeostasis. In this regard, one of the main limitations of this experiment is that TMVs were delivered to the recipient animals with a daily injection, in comparison with the continuous perfusion occurring in the tumour hosts, resulting in differences in the kinetics of exposure.

The present study assessed sncRNAs contained into MVs isolated from C26 cell culture medium or from the plasma of mice bearing the C26 tumour. Strikingly, only three miRs were differentially expressed in MVs isolated from the circulation of the C26 hosts compared with control mice, and only miR-375-3p was confirmed to be down-regulated. This miR behaves as a tumour suppressor targeting oncogenes and inhibiting proliferation in hepatocellular carcinomas, colorectal, gastric, and cervical cancers.[30] Reduced hepatic miR-375-3p was reported to activate the TGF-β1/Smad system through JAK2/STAT3. The same signalling pathways were activated in the muscle of the C26-bearing mice,[31] being potentially consistent with the reduced amount of miR-375-3p in circulating MVs.

The sncRNA profile of C26-MVs is markedly different from that assessed in MVs circulating in C26-bearing mice. This observation clearly demonstrates that tumour cells may behave quite differently *in vitro* and *in vivo*, corroborating that data deriving from cell cultures might not reflect pre-clinical results. In addition, MVs in the bloodstream derive from the tumour, but also from other cell types, including those pertaining to the inflammatory response, adipocytes, hepatocytes and myofibres themselves. In this regard, TMVs in the circulation could be diluted, resulting in concentrations of specific sncRNAs below the detection limit.

The most abundant miRs contained in MVs isolated from C26 cell cultures are miR-21a-5p, let-7i-5p, and let-7c-5p. Up-regulation of miR-21 was reported in both aged muscles and satellite cells as well as in the presence of oxidative stress or pro-inflammatory cytokines.[20] Consistently with the results shown in this study, miR-21 was proposed to act as a negative regulator of *in vitro* myogenesis. Indeed, its inhibition by a specific anti-miR was able to abrogate the impaired myogenesis induced in primary myoblasts by IL-6 or TNFα treatment.[32] As for miRs of the let family, let-7i-5p overexpression in adipocyte cultures resulted in decreased UCP1 mRNA levels and oxygen consumption, without affecting mitochondrial biogenesis and mitochondrial content.[33] At present, no data involve this miR in muscle homeostasis; however, it is a credible candidate to at least partially explain the reduced oxygen consumption observed in TMV-exposed myotubes. Also, let-7c-5p was suggested to play a role in energy metabolism, because it belongs to the HypoxamiR family and appears to regulate hypoxia likely impinging on energy production.[34]

In addition to miR expression levels, the sRNA-Seq also detected a large variety of read counts corresponding to snoRNAs, a group of short, mostly nucleoli-localized ncRNAs. They form stable and catalytically active ribonucleoprotein structures which generate either 2-*O*-methylations or pseudouridylations to target rRNAs and snRNAs.[35] Recent evidence indicates that snoRNAs contribute to regulate the alternative splicing of mRNAs and they are broadly studied as both tumour suppressors and oncogenes.[36] One predicted snoRNA, Gm23011, was found elevated in MVs circulating in C26 hosts. At present, there are almost no data in the literature linking snoRNAs to muscle homeostasis. A report published few years ago showed that SNORD114.1 was up-regulated by exercise in human volunteers.[37] In addition, snoRNAs were proposed to activate protein kinase RNA-activated (PKR),[38] previously shown to induce muscle protein degradation and reduce protein synthesis by increasing the levels of phosphorylated eIF2α. The same study also reported that both active PKR and p-eIF2α were increased in the muscle of cancer patients.[39] Consistently, pharmacological inhibition of PKR was shown to improve lipopolysaccharide-induced muscle atrophy in healthy mice.[40]

The results here reported demonstrate that TMVs retain the potential to modulate myogenesis and energy metabolism in myocyte cultures and can recapitulate some of the typical features of cachexia when infused into healthy animals. The mechanisms underlying such effects are still not clear; however, TMVs contain several sncRNAs that could actively contribute to generate the observed phenotype. In this regard, the overexpression of miR-181a-5p, miR148a-3p, or miR-21-5p into C2C12 myoblasts revealed able to down-regulate the mRNA levels of genes coding for MyHC, mainly *Myh7*, suggesting that at least these miRs could contribute to the delayed differentiation observed in C2C12 cultures exposed to TMVs. In particular, miR-181-5p was described to improve mitochondrial quality and muscle function by modulating autophagy/mitophagy in the skeletal muscle of aged animals,[41] suggesting that the effect of this specific miR might differ between differentiating myoblasts and fully differentiated myotubes. On the whole, these results demonstrate that in addition to humoral mediators produced either by the tumour of by immune cells, cancer cells use MVs as an additional mean to transmit specific signals to muscle cells, contributing to the atrophic phenotype characterizing cancer cachexia. Along this line, TMVs could become one of the potential targets of anti-cachexia strategies that could be designed to include tools able to modulate MV secretion and/or fusion with myofibres or to antagonize specific sncRNAs vehicle by TMVs.

Acknowledgements

The authors of this manuscript certify that they comply with the ethical guidelines for authorship and publishing in the *Journal of Cachexia, Sarcopenia and Muscle*.

Conflict of interest

All authors declare that they have no conflict of interest.

Funding

This work is supported by University of Torino (local research grants to P. Costelli and F. Penna), Italy.

Online supplementary material

Additional supporting information may be found online in the Supporting Information section at the end of the article.

Figure S1. MV isolation protocol.
(A) Schematic representation of the sequential ultracentrifugation protocol; (B) Mean diameter of the isolated MVs; (C) Schematic representation of the computational pipeline applied in the analysis of sRNA-Seq dataset
Figure S2. Effect of C26-MV on primary myoblast cultures.
Morphological appearance of primary myoblasts isolated from both the Extensor Digitorum Longus (EDL) and the soleus, differentiated in the presence or in the absence of C26-MV for 24 h and 48 h.
Figure S3. Modulations of the mitochondrial system exerted by C26-MV or LLC-MV on differentiating C2C12 myoblasts.
(A) Amount of polarized mitochondria assessed by fluorometry after incubation with the MitoTracker Red probe; (B) PGC-1α and (C) SDH-A expression levels (quantification and western blotting representative patterns). Data (means ± SD, $n = 3$) are expressed as % of controls. Significance of the difference: $*p < 0.05$ *vs*. controls.
Figure S4. C26-MVs are internalized into C2C12 myotubes and impinge on mitochondrial polarization.
(A) Fluorescence microscopy of C2C12 myotubes stained with PKH26 and exposed to C26-MV. (B) Immunofluorescence analysis of mitochondrial depolarization (MitoTrackerRed) in C2C12 myotubes exposed or not to C26-MV.
Figure S5. Gene expression profile in the skeletal muscle of healthy mice infused with TMV.
Healthy mice were infused with (A) C26-MV or (B) AH130-MV. Data are expressed as -ΔCt (mean ± SEM, $n = 5$). Significance of the differences: $*p < 0.05$, $**p < 0.01$ *vs*. controls.
Figure S6. Digital PCR validation of miRs found modulated by RNA-Seq in the plasma of C26-bearing mice.
Data are expressed as mean ± SD (controls: n = 5, C26 hosts: $n = 6$). Significance of the differences: $*p < 0.05$ *vs*. controls.

References

1. Elzanowska J, Semira C, Costa-Silva B. DNA in extracellular vesicles: biological and clinical aspects. *Mol Oncol* 2021;**15**:1701–1714.
2. Marinho R, Alcântara PSM, Ottoch JP, Seelaender M. Role of exosomal microRNAs and myomiRs in the development of cancer cachexia-associated muscle wasting. *Front Nutr* 2017;**4**:69.
3. He WA, Calore F, Londhe P, Canella A, Guttridge DC, Croce CM. Microvesicles containing miRNAs promote muscle cell death in cancer cachexia via TLR7. *Proc Natl Acad Sci USA* 2015;**111**:4525–4529.
4. Mu X, Agarwal R, March D, Rothenberg A, Voigt C, Tebbets J, et al. Notch signaling mediates skeletal muscle atrophy in cancer cachexia caused by osteosarcoma. *Sarcoma* 2016;**2016**:3758162.
5. Zhang G, Liu Z, Ding H, Zhou Y, Doan HA, Sin KWT, et al. Tumor induces muscle wasting in mice through releasing extracellular Hsp70 and Hsp90. *Nat Commun* 2017;**8**:589.
6. Hu W, Ru Z, Zhou Y, Xiao W, Sun R, Zhang S, et al. Lung cancer-derived extracellular vesicles induced myotube atrophy and adipocyte lipolysis via the extracellular IL-6-mediated STAT3 pathway. *Biochim Biophys Acta - Mol Cell Biol Lipids* 2019;**1864**:1091–1102.
7. Argilés JM, Busquets S, Stemmler B, López-Soriano FJ. Cancer cachexia: understanding the molecular basis. *Nat Rev Cancer* 2014;**14**:754–762.
8. Shum AMY, Poljak A, Bentley NL, Turner N, Tan TC, Polly P. Proteomic profiling of skeletal and cardiac muscle in cancer cachexia: alterations in sarcomeric and mitochondrial protein expression. *Oncotarget* 2018;**9**:22001–22022
9. Pin F, Busquets S, Toledo M, Camperi A, Lopez-Soriano FJ, Costelli P, et al. Combination of exercise training and erythropoietin prevents cancer-induced muscle alterations. *Oncotarget* 2015;**6**:43202–43215.
10. Ballarò R, Beltrà M, De Lucia S, Pin F, Ranjbar K, Hulmi JJ, et al. Moderate exercise in mice improves cancer plus chemotherapy-induced muscle wasting and mitochondrial alterations. *FASEB J* 2019;**33**:5482–5494.
11. Barreto R, Mandili G, Witzmann FA, Novelli F, Zimmers TA, Bonetto A. Cancer and chemotherapy contribute to muscle loss by activating common signaling pathways. *Front Physiol* 2016;**7**:1–13.
12. Van Niel G, D'Angelo G, Raposo G. Shedding light on the cell biology of extracellular vesicles. *Nat Rev Mol Cell Biol* 2018;**19**:213–228.
13. Goodman CA, Mabrey DM, Frey JW, Miu MH, Schmidt EK, Pierre P, et al. Novel insights into the regulation of skeletal muscle protein synthesis as revealed by a new nonradioactive in vivo technique. *FASEB J* 2011;**25**:1028–1039.
14. Sabo AA, Birolo G, Naccarati A, Dragomir MP, Aneli S, Allione A, et al. Small non-coding RNA profiling in plasma extracellular vesicles of bladder cancer patients by next-generation sequencing: expression levels of miR-126-3p and piR-5936 increase with higher histologic grades. *Cance*. MDPI AG 2020;**12**:1507.
15. Eisenberg E, Levanon EY. Human housekeeping genes, revisited. *Trends Genet* 2013;**29**:569–574.
16. Penna F, Costamagna D, Fanzani A, Bonelli G, Baccino FM, Costelli P. Muscle wasting and impaired myogenesis in tumor bearing mice are prevented by ERK inhibition. *PLoS ONE* 2010;**5**:e13604.
17. Talbert EE, Yang J, Mace TA, Farren MR, Farris AB, Young GS, et al. Dual inhibition of MEK and PI3K/Akt rescues cancer cachexia through both tumor-extrinsic and -intrinsic activities. *Mol Cancer Ther* 2017;**16**:344–356.
18. Sin J, Andres AM, Taylo RDJR, Weston T, Hiraumi Y, Stotland A, et al. Mitophagy is required for mitochondrial biogenesis and

myogenic differentiation of C2C12 myoblasts. *Autophagy* 2016;**12**:369–380.
19. Tessitore L, Bonelli G, Baccino FM. Early development of protein metabolic perturbations in the liver and skeletal muscle of tumour-bearing rats. A model system for cancer cachexia. *Biochem J* 1987;**241**:153–159.
20. Lam NT, Gartz M, Thomas L, Haberman M, Strande JL. Influence of microRNAs and exosomes in muscle health and diseases. *J Muscle Res Cell Motil* 2020;**41**:269–284.
21. Xiao R, Ferry AL, Dupont-Versteegden EE. Cell death-resistance of differentiated myotubes is associated with enhanced anti-apoptotic mechanisms compared to myoblasts. *Apoptosis* 2011;**16**:221–234.
22. Dehkordi HM, Tashakor A, O'Connell E, Fearnhead HO. Apoptosome-dependent myotube formation involves activation of caspase-3 in differentiating myoblasts. *Cell Death Dis* 2020;**11**:308.
23. Guescini M, Maggio S, Ceccaroli P, Battistelli M, Annibalini G, Piccoli G, et al. Extracellular vesicles released by oxidatively injured or intact C2C12 myotubes promote distinct responses converging toward myogenesis. *Int J Mol Sci* 2017;**18**:2488.
24. Bittel DC, Jaiswal JK. Contribution of extracellular vesicles in rebuilding injured muscles [Internet]. *Front Physiol* 2019;**10**:828.
25. Lautaoja JH, Pekkala S, Pasternack A, Laitinen M, Ritvos O, Hulmi JJ. Differentiation of murine C2C12 myoblasts strongly reduces the effects of myostatin on intracellular signaling. *Biomolecules* 2020;**10**:695.
26. Cao H, Cheng Y, Gao H, Zhuang J, Zhang W, Bian Q, et al. In vivo tracking of mesenchymal stem cell-derived extracellular vesicles improving mitochondrial function in renal ischemia-reperfusion injury. *ACS Nano* 2020;**14**:4014–4026.
27. Ma X, Wang J, Li J, Ma C, Chen S, Lei W, et al. Loading MiR-210 in endothelial progenitor cells derived exosomes boosts their beneficial effects on hypoxia/reoxygeneation-injured human endothelial cells via protecting mitochondrial function. *Cell Physiol Biochem* 2018;**46**:664–675.
28. Russell AE, Jun S, Sarkar S, Geldenhuys WJ, Lewis SE, Rellick SL, et al. Extracellular vesicles secreted in response to cytokine exposure increase mitochondrial oxygen consumption in recipient cells. *Front Cell Neurosci* 2019;**10**:695.
29. Takafuji Y, Tatsumi K, Ishida M, Kawao N, Okada K, Kaji H. Extracellular vesicles secreted from mouse muscle cells suppress osteoclast formation: Roles of mitochondrial energy metabolism. *Bone* 2020;**134**:115298.
30. Yan JW, Lin JS, He XX. The emerging role of miR-375 in cancer. *Int J Cancer* 2014;**135**:1011–1018.
31. Bonetto A, Aydogdu T, Kunzevitzky N, Guttridge DC, Khuri S, Koniaris LG, et al. STAT3 activation in skeletal muscle links muscle wasting and the acute phase response in cancer cachexia. *PLoS ONE* 2011;**6**:e22538.
32. Borja-Gonzalez M, Casas-Martinez JC, McDonagh B, Goljanek-Whysall K. Inflamma-MiR-21 negatively regulates myogenesis during ageing. *Antioxidants (Basel)* 2020;**9**:345.
33. Giroud M, Karbiener M, Pisani DF, Ghandour RA, Beranger GE, Niemi T, et al. Let-7i-5p represses brite adipocyte function in mice and humans. *Sci Rep* 2016;**6**:28613.
34. De Santi C, Melaiu O, Bonotti A, Cascione L, Di Leva G, Foddis R, et al. Deregulation of miRNAs in malignant pleural mesothelioma is associated with prognosis and suggests an alteration of cell metabolism. *Sci Rep* 2017;**7**:3140.
35. Kufel J, Grzechnik P. Small nucleolar RNAs tell a different tale. *Trends Genet* 2019;104–117.
36. Liang J, Wen J, Huang Z, Chen X, Zhang B, Chu L. Small nucleolar RNAs: insight into their function in cancer. *Front Oncol* 2019;**9**:587.
37. Håkansson KEJ, Sollie O, Simons KH, Quax PHA, Jensen J, Nossent AY. Circulating small non-coding RNAs as biomarkers for recovery after exhaustive or repetitive exercise. *Front Physiol* 2018;**9**:1136.
38. Osama AY, Sarah AS, Takahisa N, David AN, Gökhan SH, Brenda LB. Potential role for snoRNAs in PKR activation during metabolic stress. *Proc Natl Acad Sci U S A* 2015;**112**:5023–5028.
39. Eley HL, Skipworth RJE, Deans DAC, Fearon KCH, Tisdale MJ. Increased expression of phosphorylated forms of RNA-dependent protein kinase and eukaryotic initiation factor 2α may signal skeletal muscle atrophy in weight-losing cancer patients. *Br J Cancer* 2008;**98**:443–449.
40. Valentine RJ, Jefferson MA, Kohut ML, Eo H. Imoxin attenuates LPS-induced inflammation and MuRF1 expression in mouse skeletal muscle. *Physiol Rep* 2018;**6**:e13941.
41. Goljanek-Whysall K, Soriano-Arroquia A, McCormick R, Chinda C, McDonagh B. miR-181a regulates p62/SQSTM1, parkin, and protein DJ-1 promoting mitochondrial dynamics in skeletal muscle aging. *Aging Cell* 2020;**19**:e13140.